RAPID COMMUNICATIONS

PHYSICAL REVIEW B VOLUME 52, NUMBER 4 15 JULY 1995-II

Spin dynamics of triplet photoexcitations in C_{60}: Evidence for a dynamic Jahn-Teller effect

Xing Wei and Z. Valy Vardeny
Department of Physics, University of Utah, Salt Lake City, Utah 84112
(Received 4 November 1994; revised manuscript received 17 April 1995)

We have used the absorption-detected magnetic-resonance (ADMR) technique to study the spin dynamics of triplet photoexcitations in C_{60} molecules dispersed in polystyrene glasses. We found that the ADMR spectra contain two triplet powder patterns A and B with substantial spin reorientation dynamics, which increases with the temperature. The spin dynamics of triplet A are successfully modeled by a dynamic Jahn-Teller effect, where the spin reorientation process is among six degenerate D_{5d} deformations of the excited C_{60} molecule. Triplet B, however, is extrinsic in origin, with substantially different spin dynamics.

The third allotrope of carbon, the fullerenes, and, in particular, C_{60}, have recently attracted considerable theoretical and experimental interest. An important feature of C_{60} is the possession of the highest point-group symmetry, the icosahedral (I_h), which makes the electronic excited states readily subject to the Jahn-Teller (JT) effect[1] caused by vibronic coupling. The first excited electronic state of C_{60} (the t_{1u}) is triply degenerate, and its vibronic coupling with the eight JT-active h_g mode may result in JT distortions in both photoexcited C_{60} (C_{60}*) and charged C_{60}^{n-} molecules, respectively.[2–4] In some models[5] the JT effect in C_{60}^{3-} is considered to be the dominant pairing mechanism responsible for the high-T_c superconductivity in alkali-metal (A) doped compounds (A_3C_{60}).

Recent theoretical calculations[3,4,6] have suggested that the JT deformation of the lowest excited state of C_{60} is of D_{5d} symmetry, with six degenerate distortions along the directions of the six pairs of opposite pentagonal faces on the C_{60} molecule. Quantum fluctuations among the six degenerate JT distortions have been postulated to lead to dynamic JT effects[6] (DJTE), such as pseudorotation associated with Berry phase,[7] and striking modifications of the Raman and ir multiphonon spectra.[6,8] However, so far these effects have not been experimentally verified. One way to study the nature of the C_{60} JT deformations is by electron spin resonance (ESR), as was done before for the JT deformations associated with spin $\frac{1}{2}$ Ag^{2+} and Cu^{2+} impurities in MgO and CaO crystal hosts, respectively.[9] However, C_{60} molecules are spinless in the ground state, and, upon doping, the spin dynamics of C_{60}^{n-} ions may be hampered by disorder introduced into the lattice by the alkali-metal dopants. Therefore, light-induced ESR (LESR) of the long-lived triplet photoexcitations may be the cleanest way to study the JT effects in C_{60}. Although there have been several recent LESR studies of $^3C_{60}$*,[10] where spin dynamics has been recognized,[11–13] these studies have not been directly used to study the JT effect in C_{60}.

In this work we have elucidated the spin dynamics of triplet photoexcitations in C_{60} molecules dispersed in a polystyrene (PS) matrix, using the technique of absorption-detected magnetic-resonance (ADMR).[14] We found clear evidence of a DJTE in $^3C_{60}$*, in which the triplet spin dynamics are dominated by reorientation among degenerate JT deformations. To our knowledge, this is the first time that a DJTE is actually observed for spin triplet excitations,[15] which makes C_{60} quite unique.

The ADMR technique[14] uses a cw pump beam (from an Ar^+ laser) and a probe beam (from a tungsten lamp) to constantly illuminate the sample, which is mounted in a high-Q microwave cavity (at 3 GHz) equipped with optical windows, and a superconducting magnet producing a field H. Microwave resonant absorption, modulated at 500 Hz, leads to small changes, δT, in the probe transmission T. δT is proportional to δn, the change in the photoexcitation density n produced by the pump. δn is induced by transitions in the microwave range that change spin-dependent recombination rates. Here we focus on the H-ADMR spectrum in which δT is measured at a fixed probe wavelength λ, while sweeping H.

Purified C_{60} powder (with purity >99.9%) from the MER Corporation was mixed with PS in a solution of degassed toluene, which was subsequently evaporated to form C_{60}:PS glass.

The photophysics of C_{60} molecules is relatively well understood. Upon photoexcitation, a singlet exciton is formed; it subsequently decays within 5 ns into the triplet manifold, with $^3T_{1g}$ being the lowest level with a lifetime of order 1 ms.[10] Steady-state spectroscopies of C_{60} such as cw photomodulation (PM), in which the excited-state absorption is measured, show, therefore, the absorption of $^3C_{60}$*.[14,16] Figure 1 shows the PM spectrum of $^3C_{60}$* in a C_{60}:PS glass sample at temperature $\theta = 5$ K; T and ΔT are the transmission and its photoinduced changes, respectively. The $^3C_{60}$* absorption spectrum is the same as reported earlier;[10,16] it contains a strong band at 1.65 eV and a shoulder at 1.8 eV. The triplet photoexcitations decay monomolecularly, and a single lifetime of 2.5 ms is obtained from the Lorentzian shape of the in-phase and out-of-phase modulation frequency dependences of the PM signal (Fig. 1 inset).

The H-ADMR spectra of $^3C_{60}$* at various temperatures, measured at a probe photon energy of 1.65 eV, are shown in Fig. 2(a); the same spectra were obtained at other photon energies within the $^3C_{60}$* absorption bands.[16] At 2 K, the ADMR spectrum shows a 250-G-wide triplet powder pattern around $g \approx 2$ (1071 G) with $\delta n/n = -6 \times 10^{-3}$. The triplet-powder-pattern spectrum (TPPS) contains four singularities:

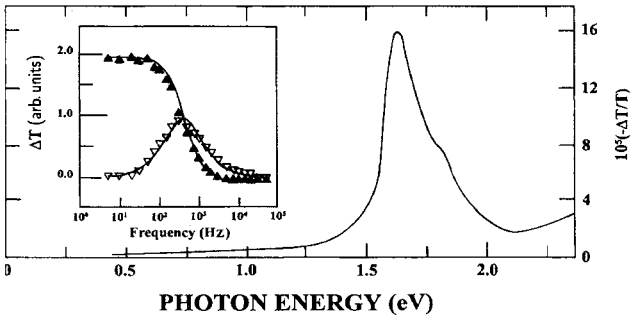

FIG. 1. The PM spectrum of $^3C_{60}$* in C_{60}:PS glass at 5 K. The inset shows the modulation frequency dependence of the 1.65-eV band at 2 K; solid triangles, in phase; open triangle, out of phase. The solid lines in the inset are a theoretical fit with a single triplet lifetime of 2.5 ms.

two steplike wings, and two peaks which are separated by $\Delta H_{12}=122$ G. All these features are due to one triplet, triplet A (T_A). Even at 2 K the two peaks in the magnetic spectrum are quite broad with full width at half maximum $2\Gamma\simeq 28$ G. The broadening mechanism at 2 K might be due to inhomogeneity in the triplet zero-field splitting (ZFS) parameters D and E.[13,16] As the temperature θ increases [Fig. 2(a)], the ADMR signal weakens as $1/\theta$ and the two peaks in the TPPS further broaden and shift towards the middle of the spectrum (at $H_0=1071$ G); hence, with increasing θ, Γ increases, ΔH_{12} decreases, and the TPPS collapses towards H_0. Moreover, a new pair of ADMR peaks belonging to a second triplet, triplet B (T_B), with smaller separation ΔH_{12} emerges. With increasing θ, T_B gains strength relative to T_A.

The apparent correlation in the T_A TPPS between ΔH_{12} and Γ with increasing θ [Fig. 2(a)] can be more directly plotted without involving θ to show that a spin dynamic process is dominant down to 2 K [Fig. 2(b)]. The straight dotted line in Fig. 2(b) is given by

$$13.7(\Gamma)^2=(125)^2-(\Delta H_{12})^2, \tag{1}$$

and fits the data reasonably well.

In the widely used Anderson spin-exchange narrowing model,[17] where the magnetic system can resonate at fields H_1 or H_2, with $\Delta H_{12}(0)=H_2-H_1$, we find

$$8(\Gamma-\Gamma_0)^2=[\Delta H_{12}(0)]^2-(\Delta H_{12})^2, \tag{2}$$

where Γ_0 is the intrinsic linewidth, and the measured linewidth Γ is larger than Γ_0 because of the exchange interaction, with $\Gamma-\Gamma_0\propto\nu$, where ν is the exchange frequency, which usually increases with θ. The similarity between the experimentally determined relation [Eq. (1)] and Eq. (2) shows that similar spin dynamics occur in $^3C_{60}$*. The 13.7 coefficient found in Eq. (1), however, indicates that the TPPS collapses towards H_0 faster than predicted by the Anderson model [Eq. (2)], showing that more complicated spin dynamics exist in $^3C_{60}$*.

To understand the spin dynamics in $^3C_{60}$*, we have considered the possibility that the triplet spin undergoes a continuous rotational diffusion on the fullerene surface.[12] However, as seen in Fig. 2(b) (broken line), we found that *the TPPS collapses too slowly with increasing* Γ *and does not fit*

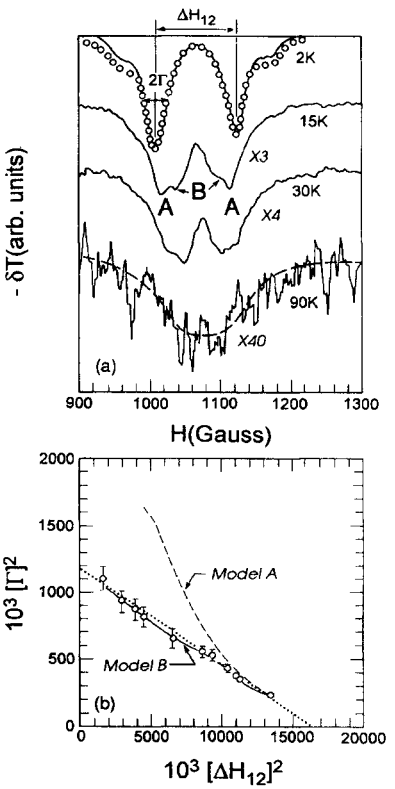

FIG. 2. (a) The H-ADMR spectra of $^3C_{60}$* at various temperatures. A and B stand for triplets T_A and T_B, respectively. The linewidth 2Γ and peaks separation ΔH_{12} in the powder patterns of T_A are indicated. A fit to the powder pattern of T_A at 2 K is shown (open circles). The dashed line through the 90-K data is a guide to the eye. (b) The correlation between Γ and ΔH_{12} in the powder patterns of T_A at various θ. The dotted line is a straight line fit [Eq. (1)], the broken line (model A) is calculated using the continuous rotational diffusion model (Ref. 12), and the full line (model B) is calculated using the DJTE model (see text).

the data. We also found that a large hopping angle ($>30°$) between the directions of the triplets involved in the spin reorientation dynamics was needed to correctly describe the TPPS collapse with Γ. This indicates that several degenerate JT deformations of $^3C_{60}$* with large reorientation angle are involved in the spin-dynamics process. As mentioned above, theory predicts[6,8] that there are six equivalent $^3C_{60}$* JT deformations with D_{5d} symmetry along the directions of the six pairs of pentagonal faces on the fullerene surface.[6,8] We then assume that the principal axis of the triplet ZFS tensor is diagonal along each of the uniaxial JT deformation, but can change its direction with respect to the external magnetic field $\vec{H}$ by hopping onto the other five equivalent JT deformations. This hopping is caused by tunneling, giving rise to a DJTE among the six degenerate JT minima in the vibronic adiabatic potential, with a calculated hopping angle of 43°. We used the density-matrix (ρ) formalism[18] to calculate the TPPS [$S(H)$] of T_A with various hopping rate (ν) at each θ. In this method

$$S(H)=\sum_{k=1}^{6}\sum_{l=1}^{3}\int \mathrm{Im}[\rho_k^l(\Omega,H)]d\Omega, \tag{3}$$

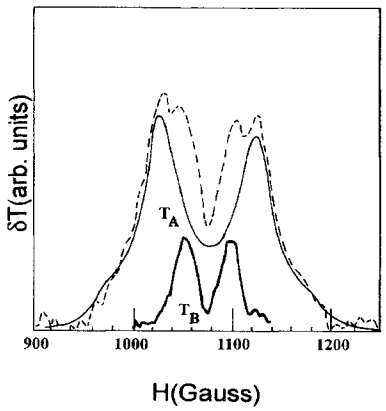

FIG. 3. H-ADMR spectrum of $^3C_{60}$* at 17 K (dashed line), showing the decomposition of the data into two triplet powder patterns: T_A (thin line) and T_B (thick line).

where ρ_k^l are ρ's of the six degenerate JT distortions, respectively, with three μ-wave transitions at each, and Ω is the angle with respect to $\vec{H}$ direction. ρ_k^l are subject to the coupled equations

$$\frac{d\rho_k^l}{dt}(\Omega,H)=\rho_k^l(\Omega,H)\{ig\beta[H-H_k^l(\Omega)]/h-1/T_2-5\nu\}$$

$$+\nu\sum_{m\neq k}\rho_m^l(\Omega,H)+is_k^l(\Omega), \tag{4}$$

where T_2 is the spin-spin relaxation time, $g\beta$ are the electronic gyromagnetic parameters, $H_k^l(\Omega)$ is the static resonance field value, and $s_k^l(\Omega)$ is the steady-state transition rate. After solving Eq. (4) in steady state ($d\rho/dt=0$) we then proceeded via Eq. (3) to obtain the TPPS of T_A.

A typical fit to the H-ADMR spectrum at $\theta=2$ K, where only T_A has been observed, is shown in Fig. 2(a). The fit was obtained with the ZFS parameters $D_A=123$ G, $E_A=0$,[19] hopping rate $\nu=2$ MHz, and $1/T_2=6$ G. Another fit to the TPPS of T_A is shown in Fig. 3, at $\theta=17$ K. The fit was obtained with the same parameters as those at $\theta=2$ K but with $\nu=7$ MHz. From the fits to the T_A ADMR spectra at various θ we found that ν linearly depends on θ as shown in Fig. 4(a) and is given (in MHz) by $\nu(\theta)=1.5+0.2\theta$; this dependence is in agreement with a one-phonon process. The full line in Fig. 2(b) shows the Γ^2 (ΔH_{12}^2) that we obtained by fitting the T_A TPPS at each temperature using the DJTE model [Eqs. (3) and (4)]. In contrast to the continuous rotational diffusion model,[12] the DJTE model fits the data very well.

Figure 3 also shows that we can readily obtain the TPPS of T_B by subtracting the fitted TPPS of T_A from the measured one. Then the TPPS of T_B (Fig. 3) can be well fit using the following ZFS parameters: $D_B=64$ G and $E_B=0$.[19] From the respective T_A and T_B integrated spectra ($\tilde{T}_A$ and $\tilde{T}_B$, respectively) we obtained the relative T_B population η, where $\eta=\tilde{T}_B/\tilde{T}_A$, as a function of θ. As shown in Fig. 4(b),

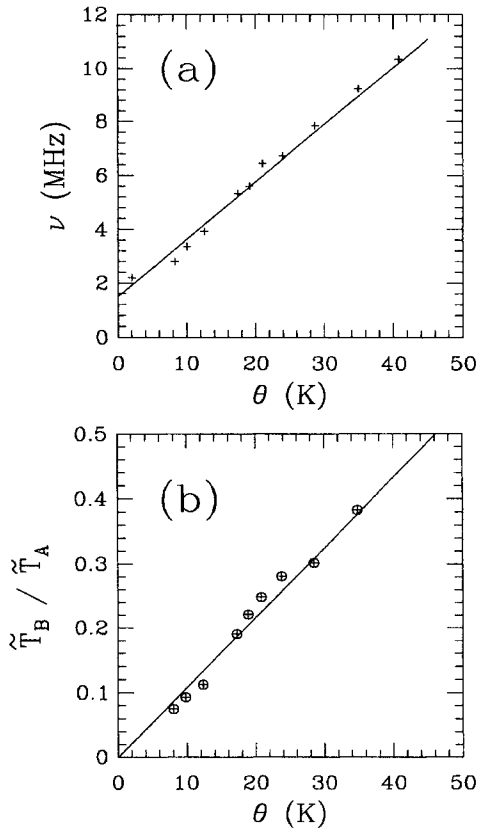

FIG. 4. The hopping frequency ν obtained from the fits of the DJTE model to the powder patterns of T_A, as a function of temperature. The line is a linear fit through the data points. (b) The relative T_B population $\eta=\tilde{T}_B/\tilde{T}_A$ as a function of temperature, obtained from the decomposition of the H-ADMR spectra into two triplet powder patterns. The straight line is a linear fit through the data points.

we found that η linearly increases with θ. We also found that triplet B too is subject to DJTE, but its two TPPS maxima collapse towards H_0 at a higher temperature compared to that of T_A.

Triplet A has been observed by several groups.[10–13,20–23] Its ZFS parameter that we found here, $D_A=123$ G ($=115\times10^{-4}$ cm^{-1}), is the same as found before in other low-temperature LESR studies.[10,13] The dynamic effects of T_A were also observed by other groups,[12] but a successful model has not been presented before. Identification of triplet B is more difficult. Since its λ-ADMR spectrum is identical to that of T_A,[16] it cannot originate from impurities; it has to be also associated with $^3C_{60}$*. The question remains, however, whether T_B is intrinsic or extrinsic in origin. Few other groups have also found a second[11,13] (sometimes even a third)[11,23] triplet in their LESR and optically detected magnetic resonance spectra of C_{60}:PS and C_{60} single crystals.[22,23] T_B ZFS parameter that we found here, $D_B=64$ G ($=60\times10^{-4}$ cm^{-1}), is well within the range of D_B found previously[11,13,22] ($47–99\times10^{-4}$ cm^{-1}). The smaller D_B and relatively larger linewidth of the T_B TPPS, compared to those of T_A, have led to the conclusion[13] that T_B is extrinsic and is formed in C_{60} aggregates, not completely dissolved by

the solvent. To check this assumption we have measured H-ADMR spectra in a variety of C_{60}:PS glasses with different C_{60} concentrations. In all cases we found two TPPS in the ADMR spectra as described here; especially the relative T_B population with θ, $\eta(\theta)$, was similar (but not identical) to that in Fig. 4(b). This may indicate that, after all, T_B is intrinsic to $^3C_{60}$*. Recent calculation of $(C_{60})^-$ JT deformations[24] has shown that several types of deformations, with different symmetries, are very close in energy (within δE of 10 cm^{-1}). These are[24] 6 equivalent D_{5d} deformations along the pentagonal faces, 10 equivalent D_{3d} deformations along the hexagonal faces, and 15 equivalent D_{2h} deformations directed towards the C-C bond in between adjacent hexagon and pentagon surface pairs. We may postulate therefore, the existence of additional types of JT deformations for $^3C_{60}$* too, with relative energies, symmetries, and degeneracies similar to those calculated for $(C_{60})^-$ (Ref. 24); we note that such calculations have not been done yet for $^3C_{60}$*.[6,8] In this model T_B can be due to $^3C_{60}$*, which is subject to a different type of JT deformation than that of T_A. Then the two $^3C_{60}$* JT populations, $\tilde{T}_A$ with D_{5d} deformation and $\tilde{T}_B$, with the other type of JT deformation, are subject to a Boltzmann distribution with θ. In this case $\eta(\theta)$ $(=\tilde{T}_B/\tilde{T}_A)$ should be thermally activated. The linear fit through the data points [Fig. 4(b)] shows, however, that such a model is incorrect.

We believe therefore that T_B is extrinsic in origin, such as due to $^3C_{60}$* in C_{60} aggregates in the sample.[13] This is in agreement with the slower T_B spin dynamics which occur at higher temperatures than those of T_A. Due to the faster T_A JT dynamics at lower temperatures, the spin-lattice relaxation rate of T_A, ν_{SL} has a stronger dependence on θ than that of T_B, for θ between 10 and 50 K, where T_B JT dynamics are practically frozen. Since $^3C_{60}$* TPPS is due to polarized spins, not to thermalized spins,[10–12] then the stronger dependence of ν_{SL} with θ decreases $\tilde{T}_A$ much more than $\tilde{T}_B$ in the ADMR spectrum. A reasonable $\nu_{SL}(\theta)$ function is a linear dependence, which consequently decreases $\tilde{T}_A$ as $1/\theta$, whereas $\tilde{T}_B$ remains constant. This explains the linear dependence of $\eta(\theta)$ shown in Fig. 4(b), without invoking a more complicated model.

In summary, the ADMR spectra of triplet photoexcitations in C_{60}:PS as a function of temperature show two triplet powder patterns, A and B, with substantial spin dynamics. The dynamics of triplet A can be explained by spin reorientation among the six degenerate JT deformations of the $^3C_{60}$* with D_{5d} symmetry. Triplet B, with lesser dynamics, is extrinsic in origin and may be due to triplets in C_{60} aggregates.

We thank A. Auerbach, H. Levanon, and W. Z. Wang for sending us copies of their papers prior to publication, and P. C. Taylor and Y. S. Wu for useful discussions. The work was supported in part by DOE Grant No. DE-FG-03-93 ER 454 90.

[1] H. A. Jahn and E. Teller, Proc. R. Soc. London Ser. A **161**, 220 (1937); C. A. Mead, Rev. Mod. Phys. **64**, 51 (1992), and references therein.

[2] F. Negri, G. Orlandi, and F. Zerbetto, Chem. Phys. Lett. **144**, 31 (1988).

[3] N. Koga and K. Morokuma, Chem. Phys. Lett. **196**, 191 (1992).

[4] W. Z. Wang, C. L. Wang, Z. B. Su, and L. Yu, Phys. Rev. Lett. **72**, 3550 (1994).

[5] C. M. Varma *et al.*, Science **254**, 989 (1991); M. Schluter *et al.*, Phys. Rev. Lett. **68**, 526 (1991).

[6] W. Z. Wang, A. R. Bishop, and L. Yu, Phys. Rev. B **50**, 5016 (1994).

[7] A. Auberbach, Phys. Rev. Lett. **72**, 2931 (1994); A. Auerbach *et al.*, Phys. Rev. B **49**, 12 998 (1994).

[8] W. Z. Wang, C. L. Wang, A. R. Bishop, L. Yu, and Z. B. Su, Phys. Rev. B **51**, 10 209 (1995).

[9] R. W. Reynolds *et al.*, Phys. Rev. B **12**, 4735 (1975); G. G. Setser *et al.*, *ibid.* **12**, 4720 (1975).

[10] Y. Kajii *et al.*, Chem. Phys. Lett. **181**, 100 (1991); T. W. Ebbesen *et al.*, *ibid.* **181**, 501 (1991); P. Lane *et al.*, Phys. Rev. Lett. **68**, 887 (1992).

[11] M. Bennati *et al.*, Chem. Phys. Lett. **200**, 440 (1992).

[12] H. Levanon *et al.*, J. Phys. Chem. **96**, 6128 (1992); A. Regev *et al.*, *ibid.* **97**, 3671 (1993).

[13] A. Angerhofer *et al.*, Chem. Phys. Lett. **217**, 403 (1994), and references therein.

[14] X. Wei, B. C. Hess, Z. V. Vardeny, and F. Wudl, Phys. Rev. Lett. **68**, 666 (1992).

[15] F. S. Ham, in *Electron Paramagnetic Resonance*, edited by S. Geschwind (Plenum, New York, 1972), p. 1.

[16] X. Wei *et al.*, Synth. Met. **54**, 273 (1993).

[17] P. W. Anderson, J. Phys. Soc. Jpn. **9**, 316 (1954).

[18] S. Alexander, J. Chem. Phys. **37**, 967 (1962); **37**, 974 (1962); J. J. Kaplan, *ibid.* **28**, 278 (1958); **29**, 462 (1958).

[19] The relatively broad TPPS leads to uncertainty in E, and we found that any $E \leq 7$ G fits well the H-ADMR spectra. Here we chose $E=0$ to reduce computation time.

[20] M. Terazima, N. Hirota, H. Shinohara, and Y. Sato, Chem. Phys. Lett. **195**, 333 (1992).

[21] G. L. Closs *et al.*, J. Phys. Chem. **96**, 5228 (1992).

[22] E. J. J. Groenen *et al.*, Chem. Phys. Lett. **197**, 314 (1992).

[23] M. Matsushita *et al.*, Chem. Phys. Lett. **214**, 349 (1993).

[24] N. Koga and K. Morokuma, Chem. Phys. Lett. **196**, 2 (1992).